



# Geophysical Research Letters

## RESEARCH LETTER

10.1029/2018GL078070

### Key Points:

- Tropospheric stratification plays a profound role in the hurricane intensity beyond the current maximum potential intensity framework
- The enhanced stabilization of the troposphere under a warming climate can significantly offset the increase in hurricane potential intensity associated with warmer SST
- Future studies of hurricane intensity variability need to take into account the variation of tropospheric stratification

### Supporting Information:

- Supporting Information S1

### Correspondence to:

C. Kieu,  
ckieu@indiana.edu

### Citation:

Kieu, C., & Zhang, D.-L. (2018). The control of environmental stratification on the hurricane maximum potential intensity. *Geophysical Research Letters*, 45, 6272–6280. <https://doi.org/10.1029/2018GL078070>

Received 27 MAR 2018

Accepted 31 MAY 2018

Accepted article online 8 JUN 2018

Published online 20 JUN 2018

## The Control of Environmental Stratification on the Hurricane Maximum Potential Intensity

Chanh Kieu<sup>1</sup>  and Da-Lin Zhang<sup>2</sup> 

<sup>1</sup>Department of Earth and Atmospheric Sciences, Indiana University, Bloomington, IN, USA, <sup>2</sup>Department of Atmospheric and Oceanic Science, University of Maryland, College Park, MD, USA

**Abstract** This study examines the dependence of the hurricane maximum potential intensity (MPI) on environmental stratification beyond the traditional MPI framework. Unlike the previous formulation in which MPI is a function of the convective available potential energy in the eyewall only, a new MPI formulation is introduced herein that explicitly incorporates the effects of environmental stratification. The new formulation is examined within an axisymmetric modeling framework, using various initial vertical thermodynamic structures. Results show the strong dependence of the model simulated maximum hurricane intensity on environmental stratification, with a lower maximum intensity for a more stable troposphere. Given the growing evidence from recent studies showing that a warmer sea surface temperature would induce a more stable troposphere, our finding suggests a smaller change in the maximum hurricane intensity in the future warming climate than that estimated from the current MPI framework. The new formulation highlights the importance of environmental stratification in hurricane development and the long-term variability of hurricane intensity, a complete understanding of which is still elusive at present.

**Plain Language Summary** This study presents a significant advance in understanding the maximum potential intensity (MPI) that a hurricane can attain in a given stratified environment. Through a series of idealized simulations in an axisymmetric framework, it is shown that environmental stratification plays a more important role in determining the MPI of hurricanes than previously thought. This finding suggests that the hurricane MPI statistics in the future warming climate is significantly overestimated, if the variation of environmental stratification is not taken into account. The opposing role of environmental stratification presented in this study provides new insights into the long-term variability of hurricane intensity beyond the traditional sea surface or upper outflow temperature proxy.

### 1. Introduction

The maximum potential intensity (MPI) that a hurricane can achieve, given sea surface temperature (SST) and outflow temperature ( $T_{OUT}$ ), as established by Emanuel (1986, 1988), is undoubtedly a key milestone in hurricane research. Such an explicit dependence of the MPI on the two key factors allows us to quantify how hurricane intensity could vary under different bottom and top boundary conditions of the troposphere, thus having an important theoretical value in current hurricane-climate research. Using SST as a key proxy, numerous studies have shown that the number of Category 4 and 5 hurricanes may increase under the future warming climate, despite overall decreases in hurricane frequency (e.g., Bengtsson et al., 2007; Knutson et al., 1998, 2007; Oouchi et al., 2006; Vecchi et al., 2013; Wang et al., 2010).

While SST is evidently a dominant factor in determining the variability of hurricane intensity (Emanuel, 2005; Knutson et al., 2007; Ramsay, 2013), extensive observational and modeling studies showed that some environmental factors may also play important roles in hurricane long-term intensity variations such as vertical wind shear (Lin & Chan, 2015; Murakami et al., 2011), midlevel moisture content (Murakami et al., 2011; Wang et al., 2010), tropical tropopause layer (Emanuel et al., 2013; Ferrara et al., 2017; Wang et al., 2014; Wing et al., 2015), or environmental stratification (EnS; Hill & Lackmann, 2011; Shen et al., 2000; Tuleya et al., 2016). Among these factors, the dependence of the MPI on EnS appears to be the least understood despite its apparent physical impacts. Namely, a more stable troposphere tends to be inimical to the development of deep convection, thereby limiting the growth of hurricane intensity as reported by a number of modeling studies. In fact, Hill and Lackmann (2011) suggested that the atmospheric stabilization in their climate projections could offset as much as 50% of the increased hurricane intensity caused by warmer SST in

the future climate. Competing effects of increased environmental stability and the warmer SST, as suggested by the previous modeling studies, motivate further examination of the role of EnS in determining the variability of hurricane intensity.

Given the potential impact of EnS on hurricane intensity, it is intriguing to see however that the current MPI framework does not explicitly contain the vertical structures of the troposphere. Except for the height dependence of equivalent potential temperature  $\theta_e$  and  $T_{OUT}$  on the moist lapse rate in the eyewall, the original MPI expression obtained by Emanuel (1986) does not fully take into account the tropospheric structures. This unaccounted role of the environmental structure in Emanuel's MPI formulation is somewhat troublesome, given that any variation in SST would inherently induce changes in environmental vertical structures of the atmosphere (e.g., Andrews & Webb, 2017; Hill & Lackmann, 2011; Larson & Hartmann, 2003) and consequently affect EnS.

Bister and Emanuel (2002, hereinafter BE02) presented an alternative MPI expression, which contains some information about atmospheric stratification in terms of convective available potential energy (CAPE) in the eyewall region. Specifically, by treating the ascending motion in the eyewall and the descending motion at the outer edge of the eyewall as two different legs of an eyewall Carnot cycle, BE02 arrived at an MPI expression as follows:

$$V_{PI}^2 = \frac{C_k}{C_d} \frac{T_s}{T_{OUT}} (CAPE^* - CAPE)|_m \quad (1)$$

where  $C_d$  and  $C_k$  are the surface drag and enthalpy exchange coefficients, respectively,  $T_s$  is the SST,  $CAPE^*$  is the CAPE of a saturated air parcel lifted from the sea level, and  $CAPE|_m$  is the CAPE of an air parcel lifted from the planetary boundary layer (PBL). Because both  $CAPE^*$  and  $CAPE|_m$  must be evaluated within the eyewall region, the term  $(CAPE^* - CAPE)|_m$  is hereafter referred to as ECAPE. The derivation of equation (1) contains some issues related to the closure of the eyewall Carnot legs (see Garner, 2015), but this formulation could at least provide a good upper bound to the MPI from climatological perspectives, despite the overall underestimation of intensity by the CAPE-MPI formulation within idealized balance framework (Bryan & Rotunno, 2009; Emanuel 2005; Garner, 2015).

Recent studies of Kieu (2015) and Kieu and Wang (2017a, hereinafter KW17, 2017b) provide a new pathway to examine MPI. By considering the basic scales of hurricanes as dynamical variables, a low-order hurricane model can be derived, which leads to an MPI limit in a different way from the original approaches that are based on either the Carnot cycle or the trajectory integration (e.g., Emanuel, 1986, 1988). Despite the simplicity of the hurricane-scale dynamics, this low-order model shows that the wind-induced surface heat exchange feedback could lead to an MPI equilibrium and its asymptotical stability, which cannot be achieved by working only with a steady state as in the previous studies.

A remarkable outcome from KW17's low-order model is an explicit dependence of the MPI on EnS beyond the ECAPE formulation. Specifically, KW17 obtained an approximated version of the MPI limit as follows:

$$V_{mPI}^2 = V_{PI}^2 [1 - \alpha(\Gamma_d - \Gamma)] \quad (2)$$

where  $\alpha$  is a proportional parameter,  $\Gamma_d = g/C_p$  is the dry lapse rate, and  $\Gamma = -dT/dz$  is the environmental lapse rate. For the sake of clarity, the subscript mPI is used in equation (2) to distinguish from  $V_{PI}$  given in equation (1). Note that  $\alpha$  is not a constant but is given by  $\alpha = H^2 g / (V_{PI}^2 T_o)$  as derived from KW17's model, where  $H$  is the scale height of the troposphere and  $T_o$  is a reference temperature. An immediate consequence of the above-modified MPI expression is that EnS, which is represented by the factor  $[1 - \alpha(\Gamma_d - \Gamma)]$ , is now explicitly contained in the MPI estimation. Basically, equation (2) indicates that the more stable the troposphere (i.e., with smaller  $\Gamma$ ), the weaker the hurricane MPI would be. This is a substantial modification to Emanuel's original MPI, because it directly includes the role of EnS in the MPI in addition to the implicit dependence of EnS hidden in the ECAPE formulation.

Due to its simplicity, KW17's hurricane-scale model could not account for the roles of eye dynamics, radiative-cloud feedbacks, cloud microphysics, or environmental conditions (e.g., vertical wind shear) in determining hurricane intensity. As a result, one may raise the following questions: How is the dependence of the model-simulated maximum intensity (i.e., the maximum surface wind,  $V_{max}$ ) on EnS realized in a

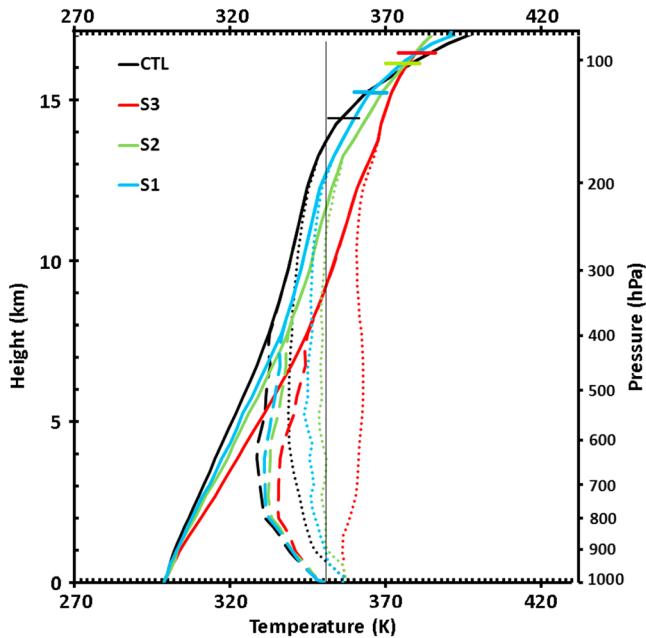


**Figure 1.** Vertical distributions of potential temperature (K, solid), equivalent potential temperature  $\theta_e$  (K, dashed), and saturated equivalent potential temperature  $\theta_e^*$  (K, dotted) that are used for the initial hurricane environments associated with four numerical experiments, in which environmental stratification is increased from the control (CTL) run given by Jordan’s (1958) sounding (black curves) to the most stable troposphere S3 run (red curves). Each colored short horizontal line denotes the tropopause level for each same-colored sounding. Horizontal axis is marked at 2-K intervals.

full-physics model compared to the KW17’s low-order hurricane model? What are the practical implications of the MPI-EnS relationship to hurricane intensity variation? How are the direct impacts of EnS on  $V_{max}$  compared to its indirect impacts via changes in ECAPE? Thus, the objective of this study is to quantify the relationship between the MPI and EnS in order to distinguish the latter’s roles from those associated with ECAPE. Because any large-scale factor that can affect the MPI will impose new constraints on the variability of hurricane intensity, addressing this objective is thus warranted.

## 2. Experiment Design

In this study, the axisymmetric Cloud Model (CM1, version 17) developed by Bryan and Fritsch (2002) is used to study the development of axisymmetric hurricanes. The capability of this model in simulating hurricane development has been well demonstrated in numerous studies (e.g., Bryan & Rotunno, 2009; Hakim, 2011, 2013; Ramsay, 2013). Our choice of this model is to take advantage of its full physics capability at the cloud-permitting resolution as well as its efficiency in simulating hurricane development for a wide range of experiments. Using the axisymmetric configurations suitable for hurricane simulations (see supporting information material for detailed model configurations), a control (CTL) experiment is first performed, using the Jordan (1958) sounding (Figure 1). Like in Rotunno and Emanuel (1987), the CTL experiment is integrated for 10 days, at which time hurricane intensity essentially approaches a quasi-steady state. The CTL-simulated  $V_{max}$  shows a 54-hr period of rapid intensification and reaches a quasi-steady state of about 70 m/s after just 4 days into the integration (Figure 2). Such rapid

approaching to the quasi-steady state confirms that the model vortex could attain its equilibrium imposed by the initial environmental conditions. As presented in e.g., Ramsay (2013), Hakim (2011), Reed and Chavas (2015), or Kieu and Moon (2016), a much longer integration shows little further changes in the characteristics of the MPI equilibrium.

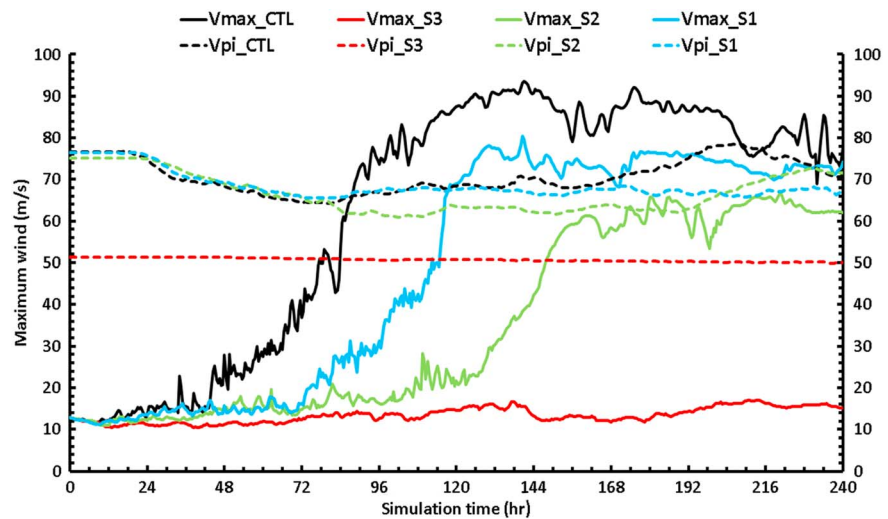


**Figure 2.** Time series of the maximum winds (solid, m/s) from four 10-day Cloud Model (CM1) simulations that are initialized with the corresponding four soundings shown in Figure 1, respectively. Dashed curves are the  $V_{pi}$  (m/s) directly computed from equation (1) at every time step, using the CM1-simulated sounding outputs of pressure, height, temperature, and specific humidity that are averaged within an annulus of radii of 500–700 km from the storm center.

With the CTL experiment, a set of 50 sensitivity experiments is conducted to examine the impacts of EnS on  $V_{\max}$  in the CM1 model by gradually decreasing the initial lapse rate  $\Gamma$  such that the static stability  $N^2 \equiv \frac{g}{\theta} \frac{\partial \theta}{\partial z} = \frac{g(\Gamma_d - \Gamma)}{\bar{T}}$  in the troposphere increases from  $\sim 1.1 \times 10^{-4} \text{ s}^{-2}$  in the CTL experiment to  $\sim 1.8 \times 10^{-4} \text{ s}^{-2}$  while maintaining approximately the same  $T_{\text{OUT}} = -73 \text{ }^\circ\text{C}$  and  $\text{SST} = 28 \text{ }^\circ\text{C}$  for this set of varying soundings (see the supporting information material for details of generating soundings with a fixed  $T_{\text{OUT}}$ ). Here the tropospheric lapse rate is defined as an averaged temperature change over the 1,000–100-hPa layer, similarly for  $N^2$ . Following the approach of Rotunno and Emanuel (1987), these soundings are then integrated until the model reaches the so-called model-neutral state under the radiative-convective equilibrium. This spinup integration approach is adopted herein, instead of integrating a model vortex for a very long time as in Ramsay (2013) and Hakim (2011, 2013) in order to circumvent the overwarming tendency emerged in a long integration related to the far-field subsidence over the entire domain for box models like the CM1.

While increasing EnS by changing the lapse rate appears to be arbitrary, we note that the environmental structures under the radiative-convective equilibrium can be affected by various factors such as gas concentration, cloudiness, moisture content, aerosols, or changes in stratospheric processes, even under the same SST condition (e.g., Iwasa et al., 2002; Lindzen, 1990; Manabe & Strickler, 1964; Manabe & Wetherald, 1967). For example, variations in ozone concentration in the stratosphere could induce changes in both the tropopause temperature and height (e.g., Manabe & Strickler, 1964; Thuburn & Craig, 2000a, 2000ab) and consequently affect EnS. In this regard, our experiment design of fixing SST while varying the environmental lapse rate can be viewed as the manifestation of different hypothetical climates in which the environmental structures are allowed to vary, even with the same SST condition.

Due to the dual roles of  $\Gamma$  in changing both CAPE and EnS, a second set of three additional sensitivity experiments is then conducted, in which the lower-tropospheric moisture content is reduced by 20% and 30% relative to the control Jordan sounding, respectively, while maintaining the same lapse rate  $\Gamma$  as in the control run. Any variation in the maximum hurricane intensity obtained in these experiments with the CM1 model can therefore reflect the relative roles of the ECAPE and EnS.

### 3. Results

#### 3.1. Effects of Environmental Stratification

Figure 2 compares the time series of the simulated  $V_{\max}$  interpolated to 10-m level, along with the theoretical  $V_{\text{PI}}$  computed by equation (1). It is evident that all developing storms exhibit similar development to that in the CTL experiment, with rapid intensification of the model vortex during the first 2–4 days, followed by a quasi-steady stage. Like the results in Shen et al. (2000), Hill and Lackmann (2011), and Tuleya et al. (2016), the CM1-simulated storms have a weaker  $V_{\max}$  for a more stable troposphere, that is, a smaller lapse rate  $\Gamma$ . For a sufficiently stable troposphere (i.e., experiment S3 with  $\Gamma \sim 5.2 \text{ K/km}$ ), CM1 could not intensify its model vortex at all, despite the same SST as those used in all the other experiments.

Of interest is that the  $V_{\text{PI}}$  estimated from equation (1) could capture a number of features comparable to  $V_{\max}$  during the quasi-steady stage, even though the former is solely based on the sounding output at each time step whereas  $V_{\max}$  denotes the maximum intensity limit obtained from the CM1 model. Specifically, the theoretical  $V_{\text{PI}}$  values vary  $\sim 16\%$  between those from the initial sounding ( $V_{\text{PI}} \sim 77 \text{ m/s}$ ) and those from the soundings at the quasi-steady stage ( $V_{\text{PI}} \sim 68 \text{ m/s}$ ), despite the fact that the model hurricane environment continuously changes during the integration. This is an important point, because it indicates that the  $V_{\text{PI}}$  values estimated solely from soundings could provide a plausible estimation for an MPI at the mature stage. Figure 2 also shows that the CAPE-MPI formulation could display the anticipated behaviors of  $V_{\text{PI}}$  as  $\Gamma$  changes. That is,  $V_{\text{PI}}$  tends to be lower for a smaller ECAPE as a result of a more stable troposphere (see Figure 1 herein and Figure S2 in supporting information material), indicating that the ECAPE term in  $V_{\text{PI}}$  captures part of the dependence on lapse rate.

However, there is a key difference between  $V_{\text{PI}}$  and  $V_{\max}$ . That is,  $V_{\text{PI}}$  exhibits much less variations than those of  $V_{\max}$  between the four experiments. In particular, the model  $V_{\max}$  shows no development for the very stable sounding S3, whereas  $V_{\text{PI}}$  still indicates a value of  $\sim 50 \text{ m/s}$  as shown by the red-dashed curve in

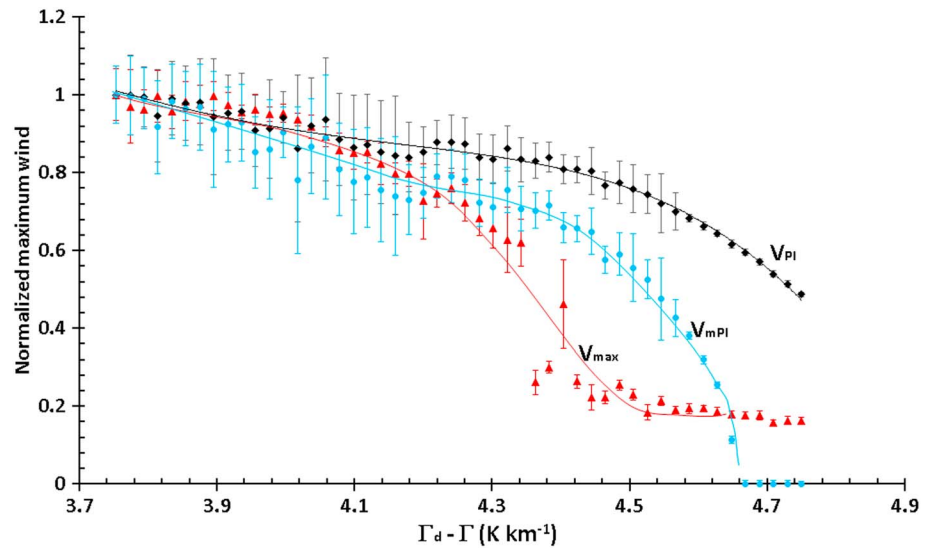


**Figure 3.** The dependence of the model-simulated  $V_{\max}$  (red triangle marks, unit m/s) on the environmental stratification factor ( $\Gamma_d - \Gamma$ ) (unit, K/km) as obtained from the 50 Cloud Model (CM1) model simulations, in which the environmental lapse rate  $\Gamma$  is decreased from the Jordan's sounding by 0.25 K/km intervals. Superimposed are the  $V_{PI}$  (black) obtained from equation (1) and  $V_{mPI}$  obtained from equation (2), using the hourly sounding output from the CM1 model simulations. Note that all values of  $V_{\max}$ ,  $V_{mPI}$ , and  $V_{PI}$  are normalized by the corresponding values with  $\Gamma = 6.5$  K/km to allow for the comparison of their functional forms (see supporting information material for details). All intensity values are averaged during the last 4 days of simulations. Error bars denote the corresponding standard deviations during the averaged period, and the solid line denotes the best polynomial fit.

Figure 2. Such a much weaker sensitivity of  $V_{PI}$  to  $\Gamma$  as compared to the model  $V_{\max}$  suggests that the ECAPE factor in the MPI formulation given by equation (1) is inadequate in characterizing the dependence of the MPI limit on EnS, even under idealized environments.

To explicitly examine the functional form of the dependence of  $V_{\max}$ ,  $V_{PI}$ , and  $V_{mPI}$  on EnS, Figure 3 shows their values for a range of  $\Gamma$  from 6.5 to 5.2 K/km. Due to the differences between the balanced formulation and the direct model output as well as the scale simplifications in KW17's low-order model, all the values of  $V_{\max}$ ,  $V_{PI}$ , and  $V_{mPI}$  in Figure 3 are normalized by those corresponding to the Jordan sounding such that only their functional forms are considered (see supporting information material for the construction of  $V_{mPI}$  from the CM1 model). It is of importance to see from Figure 3 that the relationship between  $V_{\max}$  and  $\Gamma_d - \Gamma$  is not a simple linear function but exhibits much more rapid changes of  $V_{\max}$  as  $\Gamma_d - \Gamma$  increases. For  $\Gamma < 5.5$  K/km (i.e.,  $\Gamma_d - \Gamma > 4.5$  K/km), the CM1 model could not even capture any storm development, despite the same given SST. Although  $V_{PI}$  could capture some dependence on the lapse rate via the ECAPE factor and possible dependence of  $T_{OUT}$  on the lapse rate, it is evident from Figure 3 that such dependence is substantially weaker than that of  $V_{\max}$  as obtained from the CM1 model. Specifically,  $V_{PI}$  still indicates significant TC development for the entire range of  $\Gamma$  compared to the no development for  $\Gamma < 5.5$  K/km as seen from the CM1 model. In contrast,  $V_{mPI}$  shows stronger dependence on EnS as  $\Gamma_d - \Gamma$  increases, which is consistent with equation (2). That is, a smaller lapse rate  $\Gamma$  (i.e., a more stable troposphere) corresponds to a smaller EnS factor  $[1 - \alpha(\Gamma_d - \Gamma)]$  such that  $V_{mPI}$  decreases as  $\Gamma_d - \Gamma$  increases. Thus, the additional dependence of  $V_{mPI}$  on lapse rate better captures a further decrease of  $V_{\max}$  than  $V_{PI}$  when  $\Gamma$  is reduced (Figure 3).

For a given value of  $\Gamma$  that makes the factor  $[1 - \alpha(\Gamma_d - \Gamma)] < 0$ , our modified MPI formulation dictates that no vortex intensification should occur, which is realized for  $\Gamma < 5.3$  K/km whose EnS is too stable for the model vortex to spin up (Figure 3). Of course, the dependence of  $V_{mPI}$  on  $\Gamma_d - \Gamma$ , given by equation (2), is not entirely comparable to the dependence of  $V_{\max}$  on  $\Gamma_d - \Gamma$  with substantial differences between  $V_{mPI}$  and  $V_{\max}$  for  $(\Gamma_d - \Gamma) \in [4.3 - 4.6$  K/km] as shown in Figure 3 due to the simplicity of KW17's low-order model. As such, the threshold of  $\Gamma$  at which the storm could not intensify as derived from equation (2) is different from that obtained from the CM1 model. Nevertheless, the qualitatively better fit of  $V_{mPI}$  with  $\Gamma_d - \Gamma$ , as shown in

Figure 3, indicates that EnS is an important factor in determining the maximum hurricane intensity that BE02's MPI equation (1) could not fully contain.

An immediate question with the above EnS experiments is as follows: To what degree can the initial sounding be maintained and impose subsequent impacts on the MPI limit, given the fact that ambient environment continuously changes due to both the feedback of hurricane processes and the possible environment relaxation toward a new radiative-convective equilibrium? This is an important question, because the interaction of a hurricane with its environment would likely modify the tropospheric structure that may deviate significantly from the initial vertical structure, thus rendering any estimated MPI limit, based on an initial sounding, inapplicable to the mature stage of the hurricane.

A detailed analysis of the time series of EnS for all soundings shows that all the experiments could reasonably well maintain their EnS during the 10-day integrations (Figure S1 in the supporting information material). Moreover, the relative differences of EnS among the four experiments are also preserved despite the interactions between the model vortex and environment. That is, the CTL experiment could maintain the smallest  $N^2 \sim 1.1 \times 10^{-4} \text{ s}^{-2}$  (i.e., the least stable atmosphere), while the S3 experiment persistently shows its highest value of  $N^2 \sim 1.8 \times 10^{-4} \text{ s}^{-2}$  (i.e., the most stable troposphere) throughout the 10-day integrations. Thus, this result confirms that the initial soundings could reflect the effects of EnS on the model vortex development, as expected.

Unlike the well-preserved values of  $\Gamma$ , the ECAPE varies more considerably among the four experiments as the model environment evolves (Figure S1). These variations in ECAPE translate to a fluctuation of 14–19% in  $V_{PI}$  as derived from equation (1) (see also Figure 2). In a certain sense, such large variations in the ECAPE are anticipated, because CAPE depends not only on the lapse rate  $\Gamma$  but also on the moisture of lifted air parcels. Despite these CAPE variations, it is evident that the initial soundings can impose a limit on the MPI that a hurricane can attain as a result of the dominant control of  $\Gamma$ .

### 3.2. Role of Vertical Moisture Profiles

Although we have demonstrated in the preceding subsection the role of EnS in determining the MPI, a careful examination of equation (2) shows that any change in  $\Gamma$  will affect both the ECAPE and the EnS factor  $[1 - \alpha(\Gamma_d - \Gamma)]$ . Such dual roles of EnS can be better understood, if one notes that equation (2) contains an explicit function of  $\Gamma_d - \Gamma$ , while the ECAPE dependence is a function of  $\Gamma - \Gamma_m$ , where  $\Gamma_m$  denotes the moist lapse rate. Because of this relationship, a smaller  $\Gamma$  would imply a smaller value of both the EnS factor and the ECAPE, which would in turn yield weaker MPI. Therefore, it is not conclusive from equation (2) about the relative contributions of  $\Gamma$  between these two factors, and the results shown in Figure 2 may not fully reveal the direct impacts of EnS.

Because both EnS and ECAPE may affect MPI, a third set of experiments is designed to examine the relative importance of ECAPE and EnS in equation (2). A straightforward way to varying CAPE while maintaining the same vertical temperature structure is to simply modify the vertical moisture profile. Because  $\Gamma$  is kept fixed in these moisture-varying experiments, the lifted condensation level is shifted higher for a drier profile, thus producing changes in ECAPE (see Figure S3 in supporting information material). According to equation (2), any variation of  $V_{MPI}$  in these experiments is mostly attributed to a change in the ECAPE, rather than the EnS factor  $[1 - \alpha(\Gamma_d - \Gamma)]$  because of the fixed value of  $\Gamma$ .

Figure 4 shows time series of  $V_{max}$  associated with the moisture-varying sensitivity experiments. Despite the resulting changes in the initial CAPE of ~2,855, 3,736, and 4,538 J/kg for the respective 30%, 20%, and CTL experiments as designed, it is of interest to see that the simulated  $V_{max}$  ultimately displays insignificant changes at the quasi-steady stage, which is somewhat consistent with those obtained in Persing and Montgomery (2005). The most noticeable change in  $V_{max}$  between these reduced-moisture experiments is seen during the first 120 h, after which differences in  $V_{max}$  among the sensitivity simulations appear to be indistinguishable. Another difference in these experiments is the delayed onset of rapid intensification in drier experiments; namely, a drier initial moisture structure would take a longer time for the model vortex to begin rapid intensification. This delayed intensification onset accords well with that obtained from a more realistic full-physics model (Kieu et al., 2013). Unlike  $V_{max}$ ,  $V_{PI}$  derived from equation (1) shows a larger value in an experiment with higher ECAPE in the drier initial environment experiments during the first 5-day integrations, because the drier atmospheric layer allows for a larger enthalpy difference at the surface at the initial

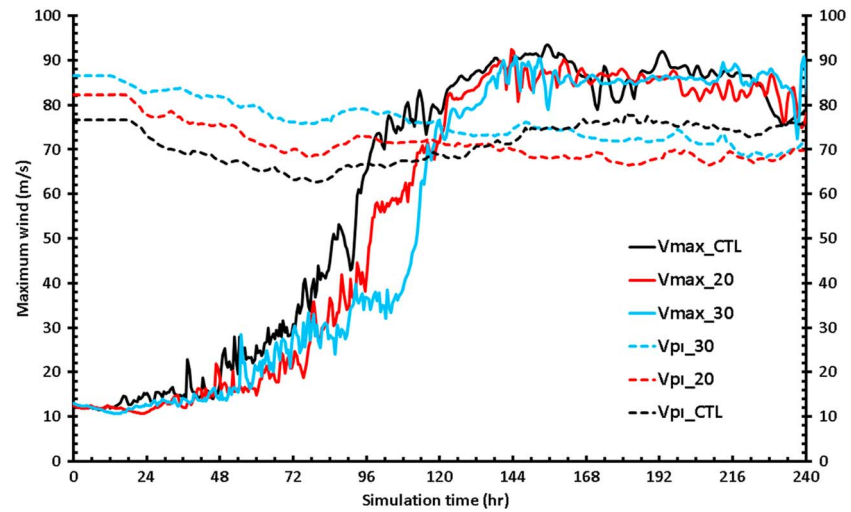


**Figure 4.** As in Figure 2, but for the moisture-varying sensitivity experiments. Colored lines denote different moisture experiments for the 30% moisture-reduction profile (blue), 20% moisture-reduction profile (red), and control (CTL) profile (black).

time. However, all the experiments eventually approach a  $V_{\max}$  limit in the range of  $\sim 80$ – $85$  m/s toward the end of the simulations.

The small differences in  $V_{\max}$  among the moisture-varying experiments highlight that the initial moisture is not well maintained with time, unlike the environmental lapse rate  $\Gamma$  in the EnS experiments. That is, the moisture profile evolves markedly during the model integration, with the lower-tropospheric moisture approaching saturation in the eyewall as the storm intensifies. As a result, the vertical moisture profiles become closer to each other in all the three moisture-varying sensitivity experiments after just 5 days into the integrations despite their initial differences. In this regard, changing the ECAPE by simply varying the moisture content while keeping  $\Gamma$  unchanged tends to produce minimum impacts on the MPI. On the contrary, changing the ECAPE through the vertical temperature structure would result in a much more profound impact on the MPI due to the well-preserved environmental structure of  $\Gamma$  during hurricane development (cf. Figures 2 and S2). The above result appears to explain the insensitivity of  $V_{\max}$  to CAPE variations shown in Figure 4, while offering insight into the strong dependence of  $V_{\max}$  on EnS.

From a thermodynamic perspective, the above insensitivity of  $V_{\max}$  can also be understood if one notes the difference between the environmental CAPE and the ECAPE (Garner, 2015). That is, it is possible to have different environmental CAPEs, while the ECAPE may remain the same values during hurricane development. Specifically, the CAPE-MPI formulation of equation (1) is only applied to hypothetical thermodynamic legs bounded by the inner and outer edges of the eyewall-induced secondary circulation. Therefore, the CAPE estimated from BE02's formulation must be evaluated near the RMW where the air is always saturated, which differs from the environmental CAPE as discussed in Garner (2015). In this regard, Persing and Montgomery (2005)'s experiments may possess similar ECAPE, thus accounting for the same MPI despite the different environmental CAPE in their experimental design. This subtle issue in the CAPE calculation is an essential feature of the CAPE-MPI formulation that may cause some confusion in practical applications.

#### 4. Concluding Remarks

In this study, a modified MPI formulation developed by Kieu and Wang (2017a, 2017b) is examined through a series of sensitivity simulations. By explicitly taking into account EnS, our modified MPI formulation allows for the incorporation of an additional factor that is proportional to the environmental lapse rate in the form of  $[1 - \alpha(\Gamma_d - \Gamma)]$ . The explicit functional form of this factor provides a systematical way to examine the dependence of the MPI on EnS with full-physics model simulations, as demonstrated in this study. Given the growing evidence of the tropospheric stabilization in response to warmer SST, it is therefore critical to understand the competing impacts between EnS and SST on the model-simulated maximum hurricane intensity.

Using the nonhydrostatic CM1 model, four sets of idealized experiments are conducted herein, in which the environmental lapse rate and lower tropospheric moisture are varied from the control Jordan sounding. Results show that increasing the lapse rate  $\Gamma$  does impose a stronger constraint on the model-simulated  $V_{\max}$  than what is dictated by Emanuel's original MPI framework. Specifically, a more stable troposphere leads to a weaker  $V_{\max}$ , even with the same SST and tropopause temperature. Furthermore, the model vortex cannot intensify if the environmental lapse rate is larger than a threshold value regardless of the initial vortex strength or radiative cooling (see supporting information material), whereas Emanuel's MPI limit still shows a value as large as 50 m/s. A series of sensitivity experiments to changing SST and initial vortex strength, presented in the supporting information materials, shows that the impact of the EnS factor is reduced as SST increases. In particular, the model can eventually spin up an initial vortex even in a very stable troposphere, provided that SST exceeds a certain limit (see Table S2 in the supporting information materials).

Because both ECAPE and the EnS factor affect  $V_{\text{MPI}}$ , additional experiments are conducted, in which the lower-level atmospheric moisture content is modified while keeping the lapse rate (and therefore the EnS factor) unchanged. Results show very similar  $V_{\max}$  among all the experiments during the quasi-steady stage. The only significant difference among these moisture-varying experiments is the onset of rapid intensification that tends to be delayed in an initially drier environment. As discussed in Kieu et al. (2013) and Tang et al. (2016), this feature can be attributed to the time required for the model to moisten the lower troposphere before the storm central region becomes saturated for deep convection to develop.

The subtle competing role of SST and EnS in determining the MPI raises an important issue about the long-term variability of hurricane intensity. At a broad level, the results from this study suggest that the variations of both SST and environmental lapse rate must be taken into account in examining the variability of hurricane intensity. Under the radiative-convective equilibrium, previous studies (Andrews & Webb, 2017; Hill & Lackmann, 2011; Larson & Hartmann, 2003) showed that an SST increase is always accompanied by increased stabilization of the troposphere. Therefore, any statistical analysis of the hurricane maximum intensity variability in the future warming climate, based on the current MPI theory without considering the impact of changing tropospheric EnS, tends to overestimate the projection of actual hurricane maximum intensity. The explicit functional dependence of the modified-MPI on EnS suggests a possible statistical relationship that one can apply to the studies of hurricane intensity variability. Detailed statistical analyses of the environmental control of EnS on the long-term variability of hurricane intensity derived from the reanalysis data will be presented in our forthcoming studies.

#### Acknowledgments

We would like to thank two anonymous reviewers, whose comments and suggestions have helped improve this work substantially, and Daniel Chavas and Tim Cronin for their various discussions related to the MPI-CAPE formulation. We would also like to acknowledge the use of the MPI-CAPE program provided by Kerry Emanuel on his webpage. This research was partially supported by the National Oceanic and Atmospheric Administration (NOAA) HFIP funding (award NA16NWS4680026), the Office of Naval Research (ONR) funding (grant N000141410143), and the ONR's Young Investigator Award. The full input data for the CM1 model that can be used to produce the results in this work is available at <http://pages.iu.edu/~ckieu/public/tc-cm1.tar.gz>.

#### References

- Andrews, T., & Webb, M. J. (2017). The dependence of global cloud and lapse-rate feedbacks on the spatial structure of tropical Pacific warming. *Journal of Climate*, 31(2), 641–654. <https://doi.org/10.1175/JCLI-D-17-0087.1>
- Bengtsson, L., KI Hodges, M., Esch, N., Keenlyside, L. K., Luo, J.-J., & Yamagata, T. (2007). How may tropical cyclones change in a warmer climate? *Tellus*, 59A, 539–561.
- Bister, M., & Emanuel, K. A. (2002). Low frequency variability of tropical cyclone potential intensity, 1. Interannual to interdecadal variability. *Journal of Geophysical Research*, 107(D24), 4801. <https://doi.org/10.1029/2001JD000776>
- Bryan, G. H., & Fritsch, J. M. (2002). A benchmark simulation for moist nonhydrostatic numerical models. *Monthly Weather Review*, 130(12), 2917–2928. [https://doi.org/10.1175/1520-0493\(2002\)130<2917:ABSFMN>2.0.CO;2](https://doi.org/10.1175/1520-0493(2002)130<2917:ABSFMN>2.0.CO;2)
- Bryan, G. H., & Rotunno, R. (2009). The maximum intensity of tropical cyclones in axisymmetric numerical model simulations. *Monthly Weather Review*, 137(6), 1770–1789. <https://doi.org/10.1175/2008MWR2709.1>
- Emanuel, K. A. (1986). An air–sea interaction theory for tropical cyclones. Part I: Steady-state maintenance. *Journal of the Atmospheric Sciences*, 43(6), 585–605. [https://doi.org/10.1175/1520-0469\(1986\)043<0585:AASITF>2.0.CO;2](https://doi.org/10.1175/1520-0469(1986)043<0585:AASITF>2.0.CO;2)
- Emanuel, K. A. (1988). The maximum intensity of hurricanes. *Journal of the Atmospheric Sciences*, 45(7), 1143–1155. [https://doi.org/10.1175/1520-0469\(1988\)045<1143:TMOH>2.0.CO;2](https://doi.org/10.1175/1520-0469(1988)045<1143:TMOH>2.0.CO;2)
- Emanuel, K. A. (2005). Increasing destructiveness of tropical cyclones over the past 30 years. *Nature*, 436(7051), 686–688. <https://doi.org/10.1038/nature03906>
- Emanuel, K. A., Solomon, S., Folini, D., Davis, S., & Cagnazzo, C. (2013). Influence of tropical tropopause layer cooling on Atlantic hurricane activity. *Journal of Climate*, 26(7), 2288–2301. <https://doi.org/10.1175/JCLI-D-12-00242.1>
- Ferrara, M., Groff, F., Moon, Z., Keshavamurthy, K., Robeson, S. M., & Kieu, C. Q. (2017). Large-scale control of the lower stratosphere on variability of tropical cyclone intensity. *Geophysical Research Letters*, 44, 4313–4323. <https://doi.org/10.1002/2017GL073327>
- Garner, S. (2015). The relationship between hurricane potential intensity and CAPE. *Journal of the Atmospheric Sciences*, 72(1), 141–163. <https://doi.org/10.1175/JAS-D-14-0008.1>
- Hakim, G. J. (2011). The mean state of axisymmetric hurricanes in statistical equilibrium. *Journal of the Atmospheric Sciences*, 68(6), 1364–1376. <https://doi.org/10.1175/2010JAS3644.1>
- Hakim, G. J. (2013). The variability and predictability of axisymmetric hurricanes in statistical equilibrium. *Journal of the Atmospheric Sciences*, 70(4), 993–1005. <https://doi.org/10.1175/JAS-D-12-0188.1>

- Hill, K., & Lackmann, G. (2011). The impact of future climate change on TC intensity and structure: A downscaling approach. *Journal of Climate*, 24(17), 4644–4661. <https://doi.org/10.1175/2011JCLI3761.1>
- Iwasa, Y., Abe, Y., & Tanaka, H. (2002). Structure of the atmosphere in radiative–convective equilibrium. *Journal of the Atmospheric Sciences*, 59(14), 2197–2226. [https://doi.org/10.1175/1520-0469\(2002\)059<2197:SOTAIR>2.0.CO;2](https://doi.org/10.1175/1520-0469(2002)059<2197:SOTAIR>2.0.CO;2)
- Jordan, C. L. (1958). Mean soundings for the West Indies area. *Journal of Meteorology*, 15(1), 91–97. [https://doi.org/10.1175/1520-0469\(1958\)015<0091:MSFTWI>2.0.CO;2](https://doi.org/10.1175/1520-0469(1958)015<0091:MSFTWI>2.0.CO;2)
- Kieu, C. Q. (2015). Hurricane maximum potential intensity equilibrium. *Quarterly Journal of the Royal Meteorological Society*, 141(692), 2471–2480. <https://doi.org/10.1002/qj.2556>
- Kieu, C. Q., & Moon, Z. (2016). Hurricane intensity predictability. *Bulletin of the American Meteorological Society*, 97(10), 1847–1857. <https://doi.org/10.1175/BAMS-D-15-00168.1>
- Kieu, C. Q., Tallapragada, V., & Hogsett, W. (2013). On the onset of the tropical cyclone rapid intensification in the HWRF model. *Geophysical Research Letters*, 9, 3298–3306. <https://doi.org/10.1002/2014GL059584>
- Kieu, C. Q., & Wang, Q. (2017a). Stability of hurricane maximum potential intensity. *Journal of the Atmospheric Sciences*, 74(11), 3591–3608. <https://doi.org/10.1175/JAS-D-17-0028.1>
- Kieu, C. Q., & Wang, Q. (2017b). On the scale dynamics of tropical cyclone intensity. *Discrete and Continuous Dynamical Systems Series B*, 22(5), 44–54. <https://doi.org/10.3934/dcdsb.2017196>
- Knutson, T. R., Sirutis, J. J., Garner, S. T., Held, I. M., & Tuleya, R. E. (2007). Simulation of the recent multidecadal increase of Atlantic hurricane activity using an 18-km-grid regional model. *Bulletin of the American Meteorological Society*, 88, 1549–1565.
- Knutson, T. R., Tuleya, R. E., & Kurihara, Y. (1998). Simulated increase of hurricane intensities in a CO<sub>2</sub>-warmed climate. *Science*, 279(5353), 1018–1021. <https://doi.org/10.1126/science.279.5353.1018>
- Larson, K., & Hartmann, D. L. (2003). Interactions among cloud, water vapor, radiation, and large-scale circulation in the tropical climate. Part I: Sensitivity to uniform sea surface temperature changes. *Journal of Climate*, 16(10), 1425–1440. <https://doi.org/10.1175/1520-0442-16.10.1425>
- Lin, I.-I., & Chan, J. C. (2015). Recent decrease in typhoon destructive potential and global warming implications. *Nature Communications*, 6(1), 7182. <https://doi.org/10.1038/ncomms8182>
- Lindzen, R. S. (1990). Some coolness concerning global warming. *Bulletin of the American Meteorological Society*, 71, 123–135.
- Manabe, S., & Strickler, R. F. (1964). Thermal equilibrium of the atmosphere with a convective adjustment. *Journal of the Atmospheric Sciences*, 21(4), 361–385. [https://doi.org/10.1175/1520-0469\(1964\)021<0361:TEOTAW>2.0.CO;2](https://doi.org/10.1175/1520-0469(1964)021<0361:TEOTAW>2.0.CO;2)
- Manabe, S., & Wetherald, R. T. (1967). Thermal equilibrium of the atmosphere with a given distribution of relative humidity. *Journal of the Atmospheric Sciences*, 24(3), 241–259. [https://doi.org/10.1175/1520-0469\(1967\)024<0241:TEOTAW>2.0.CO;2](https://doi.org/10.1175/1520-0469(1967)024<0241:TEOTAW>2.0.CO;2)
- Murakami, H., Wang, B., & Kitoh, A. (2011). Future change of western North Pacific typhoons: Projections by a 20-km-mesh global atmospheric model. *Journal of Climate*, 24(4), 1154–1169. <https://doi.org/10.1175/2010JCLI3723.1>
- Oouchi, K., Yoshimura, J., Yoshimura, H., Mizuta, R., Kusunoki, S., & Noda, A. (2006). Tropical cyclone climatology in a global-warming climate as simulated in a 20 km-mesh global atmospheric model: Frequency and wind intensity analyses. *Journal of the Meteorological Society of Japan*, 84(2), 259–276. <https://doi.org/10.2151/jmsj.84.259>
- Persing, J., & Montgomery, M. T. (2005). Is environmental CAPE important in the determination of maximum possible hurricane intensity? *Journal of the Atmospheric Sciences*, 62(2), 542–550. <https://doi.org/10.1175/JAS-3370.1>
- Ramsay, H. A. (2013). The effects of imposed stratospheric cooling on the maximum intensity of tropical cyclones in axisymmetric radiative-convective equilibrium. *Journal of Climate*, 26(24), 9977–9985. <https://doi.org/10.1175/JCLI-D-13-00195.1>
- Reed, K., & Chavas, D. R. (2015). Uniformly-rotating global radiative-convective equilibrium in the Community Atmosphere Model, version 5. *Journal of Advances in Modeling Earth Systems*, 7(4), 1938–1955. <https://doi.org/10.1002/2015MS000519>
- Rotunno, R., & Emanuel, K. A. (1987). An air–sea interaction theory for tropical cyclones. Part II: Evolutionary study using a non-hydrostatic axisymmetric numerical model. *Journal of the Atmospheric Sciences*, 44(3), 542–561. [https://doi.org/10.1175/1520-0469\(1987\)044<0542:AAITFT>2.0.CO;2](https://doi.org/10.1175/1520-0469(1987)044<0542:AAITFT>2.0.CO;2)
- Shen, W., Tuleya, R. E., & Ginis, I. (2000). A sensitivity study of the thermodynamic environment on GFDL model hurricane intensity: Implications for global warming. *Journal of Climate*, 13(1), 109–121. [https://doi.org/10.1175/1520-0442\(2000\)013<0109:ASSOTT>2.0.CO;2](https://doi.org/10.1175/1520-0442(2000)013<0109:ASSOTT>2.0.CO;2)
- Tang, B. H., Rios-Berrios, R., Alland, J. J., Berman, J. D., & Corbosiero, K. L. (2016). Sensitivity of axisymmetric tropical cyclone spinup time to dry air aloft. *Journal of the Atmospheric Sciences*, 73(11), 4269–4287. <https://doi.org/10.1175/JAS-D-16-0068.1>
- Thuburn, J., & Craig, G. C. (2000a). Stratospheric influence on tropopause height: The radiative constraint. *Journal of the Atmospheric Sciences*, 57(1), 17–28. [https://doi.org/10.1175/1520-0469\(2000\)057<0017:SIOTHT>2.0.CO;2](https://doi.org/10.1175/1520-0469(2000)057<0017:SIOTHT>2.0.CO;2)
- Thuburn, J., & Craig, G. C. (2000b). On the temperature structure of the tropical stratosphere. *Journal of Geophysical Research*, 107, 60–69.
- Tuleya, R. E., Bender, M., Knutson, T. R., Sirutis, J. J., Thomas, B., & Ginis, I. (2016). Impact of upper-tropospheric temperature anomalies and vertical wind shear on tropical cyclone evolution using an idealized version of the operational GFDL hurricane model. *Journal of the Atmospheric Sciences*, 73, 3803–3820.
- Vecchi, G. A., Fueglistaler, S., Held, I. M., Knutson, T. R., & Zhao, M. (2013). Impacts of atmospheric temperature trends on tropical cyclone activity. *Journal of Climate*, 26(11), 3877–3891. <https://doi.org/10.1175/JCLI-D-12-00503.1>
- Wang, B., Yang, Y., Ding, Q.-H., Murakami, H., & Huang, F. (2010). Climate control of the global tropical storm days (1965–2008). *Geophysical Research Letters*, 37, L07704. <https://doi.org/10.1029/2010GL042487>
- Wang, S., Camargo, S. J., Sobel, A. H., & Polvani, L. M. (2014). Impact of the tropopause temperature on the intensity of tropical cyclones: An idealized study using a mesoscale model. *Journal of the Atmospheric Sciences*, 71(11), 4333–4348. <https://doi.org/10.1175/JAS-D-14-0029.1>
- Wing, A. A., Emanuel, K. A., & Solomon, S. (2015). On the factors affecting trends and variability in tropical cyclone potential intensity. *Geophysical Research Letters*, 42, 8669–8677. <https://doi.org/10.1002/2015GL066145>